Sensors and Actuators B 187 (2013) 522–532

Contents lists available at SciVerse ScienceDirect

Sensors and Actuators B: Chemical

journal homepage: www.elsevier.com/locate/snb

Progress in NASICON-based mixed-potential type gas sensors

Xishuang Liang[a], Biao Wang[b], Han Zhang[a], Quan Diao[a], Baofu Quan[a], Geyu Lu[a,*]

[a] State Key Laboratory on Integrated Optoelectronics, College of Electronic Science and Engineering, Jilin University, 2699 Qianjin Street, Changchun 130012, China
[b] Changchun Institute of Optics, Fine Mechanics and Physics, CAS, 3888 Dong Nanhu Road, Changchun 130033, China

ARTICLE INFO

Article history:
Available online 22 March 2013

Keywords:
NASICON
Gas sensor
Oxide electrode
Mixed potential

ABSTRACT

The mixed-potential type gas sensors combining NASICON with oxide electrodes exhibit high sensing performance to typical pollution gases in the atmospheric environment in the intermediate temperature range, indicating a potential in practical application. This paper describes the state-of-the-art for the sensors based on the NASICON, including the current-type, the equilibrium-potential-type and mixed-potential-type. For improving the performance of sensors based on the NASICON and oxide electrodes, two main approaches have been utilized: the developing of new oxide electrode materials and the design of novel sensor structure for enhancing the sensing performance as well as the sensing mechanism involved in the mixed potential.

1. Introduction

With the increasing of world's population and the acceleration of the industrialization process, lots of harmful gases (CO_2, SO_x, NO_x, H_2S, NH_3, CO and so on) from the power generation, heat supplying, metallurgy, chemical production and motor vehicle lead to severe atmospheric pollution, e.g., greenhouse effect, acid rain, photochemical smog and other environmental disasters. Therefore, the high-performance environment gas sensors have been urgently desired for detecting and monitoring these hazardous gases. Up to now, various kinds of gas sensors based on semiconductor oxides [1], organic thin films [2] and solid electrolytes [3] have been developed. Among them, the solid electrolyte type sensors exhibit excellent sensing performances, such as high sensitivity, rapid response kinetics, outstanding selectivity and reproducibility. For the solid electrolyte sensors, most of researches have focused on the sensors based on yttria stablized zirconia (YSZ) and sodium super ionic conductor (NASICON) [4–8]. In general, the YSZ-based sensor was operated at elevated temperature (600–800 °C), so it seems to be inappropriate for detecting the gases in atmospheric environment because of its low sensitivity and high power consumption. Contrary to the YSZ-based sensors, the mixed potential type sensors based on NASICON are generally operated at relatively lower temperature range (100–500 °C), moreover, having novel sensing performance, so they are more suitable for detecting the hazardous gases in the atmospheric environment.

Sodium (Na) Super Ionic CONductors (NASICON) is interesting candidates for applications in solid state electrochemistry where fast ionic conductivity is required [9–16]. The crystal structure of NASICON-type phases of general formula $Na_{1+x}Zr_2Si_xP_{3-x}O_{12}$ can be described from corner-sharing of ZrO_6 octahedra and PO_4–SiO_4 tetrahedra, and Na^+ ions located at interstitial sites of the network (Fig. 1) [17,18]. The three-dimensional framework $Zr_2Si_xP_{3-x}O_{12}$ obtained delimits large cavities which can be occupied by Na^+ ions. Two main types of cavities, M_1 and M_2, are often considered: the M1 cavity, one per formula unit, is located between two ZrO_6 octahedra along the c-axis forming ribbons $O_3ZrO_3NaO_3ZrO_3$, while the M_2 cavity, three per formula unit, is situated between these ribbons. Indeed, NASICON with $Na_{1+x}Zr_2Si_xP_{3-x}O_{12}$ stoichiometry shows high Na^+ conductivity for $x=2$, and the most suitable for making gas sensor.

According to the sensing mechanism, the NASICON-based gas sensors are mainly divided into three types:

I NASICON-based the current-type sensors, researchers mainly focus on the structure and auxiliary materials of sensors.
II NASICON-based equilibrium-potential-type sensors, CO_2 sensor is the research point, including the auxiliary electrode materials, reference electrode materials and the sensing mechanism of sensors.
III NASICON-based mixed-potential type sensors, researchers place great emphasis on the improvement of oxide-sensing materials and device structure.

Besides, a few researchers reported that gas-sensing mechanism of SnO_2/NASICON composite materials and thick film electrochemical sensor based on the kinetics of the controlled chemical reaction [19–22]. This paper provides an overview and mainly expressed the state-of-the-art about the gas sensors based on NASICON solid electrolyte. For improving the performance of sensors based

* Corresponding author. Tel.: +86 431 85167808; fax: +86 431 85167808.
E-mail address: lugy@jlu.edu.cn (G. Lu).

0925-4005/$ – see front matter © 2013 Elsevier B.V. All rights reserved.
http://dx.doi.org/10.1016/j.snb.2013.03.032

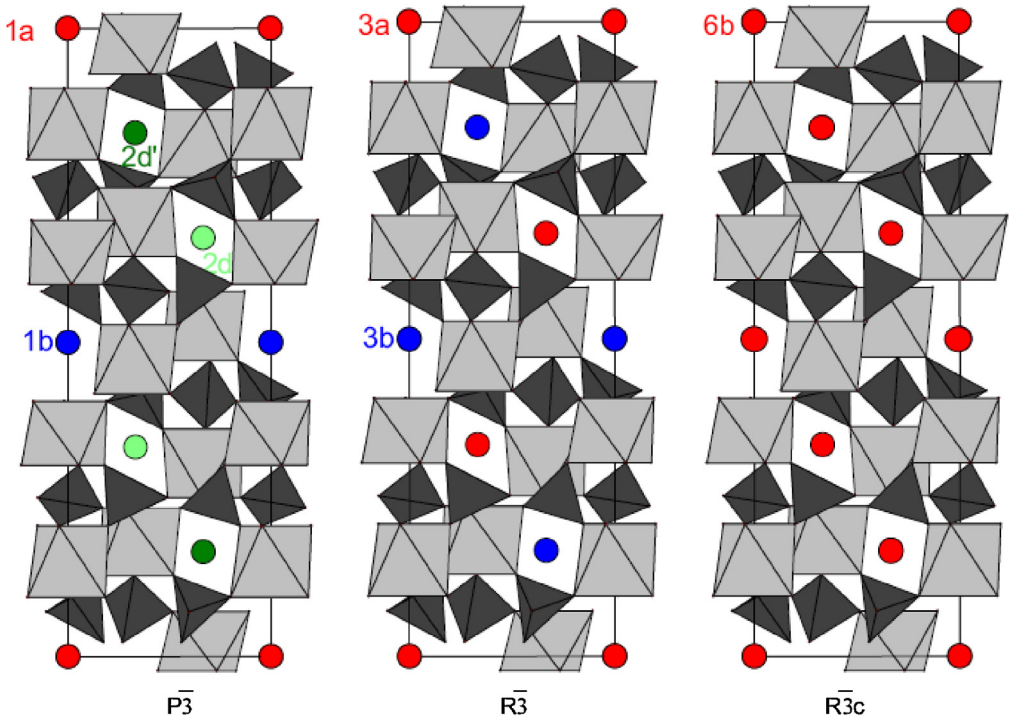

Fig. 1. Projection of the NASICON-type structure in the three space groups $\bar{P}$, $R\bar{3}$ and $R\bar{3}$ c showing the different M1 sites available for the A cations in a preserved $[Zr_2(PO_4)_3]$ framework.
Source: reprinted from Ref. [18] with permission from Elsevier.

on the NASICON and oxide electrodes, we have taken two main approaches: the developing of new oxide electrode materials and the design of novel sensor structure for enhancing the sensing performance.

2. Development of NASICON-based the current-type sensors

Generally speaking, amperometric sensors, if properly fabricated, can give more precise concentration data than potentiometric sensors. Up to now, NASICON-based the current-type sensors are mainly divided into NO_2 and CO_2 sensor [23–27], Miura et al. first utilized the NASICON-based the current-type sensors for detecting NO_2 in 1996 [24], sensor was designed by combining a Na^+ conductor (NASICON) with $NaNO_2$ (or $NaNO_3$) auxiliary layers deposited on both sensing and counter electrodes. The current response of this sensor varied linearly with NO_2 concentration (Fig. 2) [24], but its lowest limit of NO_2 detection was several-hundred ppb. In addition, the original sensor needs the flow of air to the reference electrode side as a reference gas, so the simplification and miniaturization of sensor structure are not easy. In order to overcome these drawbacks, N. Miura et al. have proposed a compact, solid-state, amperometric NO_2 sensor was fabricated using a small NASICON plate and an $NaNO_2$ layer deposited on the counter electrode. With the sensing electrode polarized at a constant potential relative to the reference Au electrode coated with an inorganic adhesive, electric current flowing through the device under exposure to NO_2 was measured as a sensing signal in 1998 [25]. The current response of sensor was almost linear with NO_2 concentration in the range 10 ppb to 1 ppm at 150 °C (Fig. 3) [25]. The 90% response time to even 20 ppb NO_2 was ca. 60 s. The NO_2 sensitivity was hardly affected by the coexistence of CO_2, H_2O and O_2. Furthermore, the device could be operated rather stably during the test period of ca. 30 days except for several days in the early stage. As for CO_2 sensor, J. Lee et al. have exerted an amperometric CO_2 sensor which was fabricated using a Pt|NASICON|Pt cell and a porous Na_2CO_3–$BaCO_3$ (1:1.7 in molar ratio) auxiliary layer in 2003 [26,27]. Fig. 4 shows the sensor signal as a function of the CO_2 concentration in dry and wet atmospheres (20 °C in dew point) [27]. The current was approximately proportional to the logarithm of the CO_2 concentration although the data at low CO_2 concentration (the dotted part in line) showed a little deviation. The presence of humidity had little effect on the amperometric signal.

3. Development of NASICON-based CO_2 equilibrium-potential-type sensors

This type of CO_2 sensor was reported firstly by Maruyama et al. in 1986 [28], who combined a NASICON-based cell with a Na_2CO_3

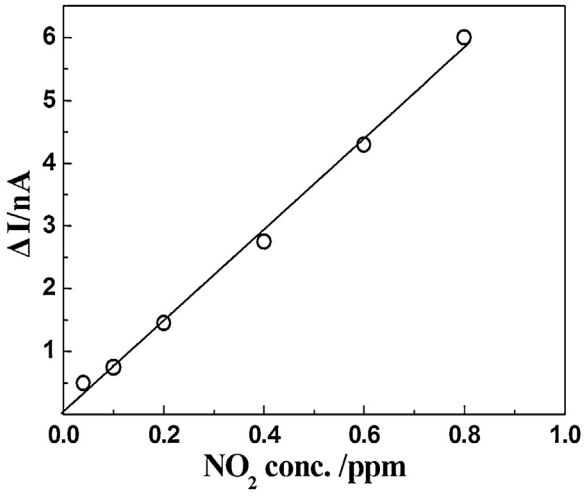

Fig. 2. Dependence of the $NaNO_2$-attached device on NO_2 concentration at 200 °C.
Source: reprinted from reference [24] with permission from Elsevier.

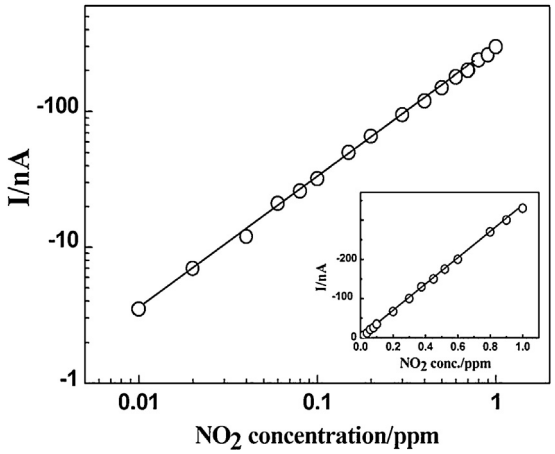

Fig. 3. Dependence of current value on NO_2 concentration in air for the compact amperometric sensor at 150 °C. (The sensing electrode potential: 150 mV vs. the reference Au electrode.)

Source: reprinted from reference [25] with permission from Elsevier.

auxiliary phase. And then, a number of investigators have shown that sensor properties can be upgraded by replacing Na_2CO_3 with a binary carbonate system such as Na_2CO_3–$BaCO_3$ and Li_2CO_3–$BaCO_3$ [29–34,38–47]. For example, Yamazoe et al. reported a simple potentiometric CO_2 sensor based upon NASICON was found to be greatly improved in response time and water vapor-resistance by using a binary carbonate electrode of $BaCO_3$–Na_2CO_3. The response of this sensor was perfectly linear to the logarithm of CO_2 concentration in the whole range tested (4–400,000 ppm) with a Nernst's lope of 81 mV/decade, water vapor hardly affected the sensor characteristics, in contrast to the case of a pure Na_2CO_3 electrode, with a 90% response time of as short as 8 s [30].

Subsequent examinations from a practical viewpoint, however, disclosed that these electrodes ($BaCO_3$–Na_2CO_3, etc.) were not stable enough during storage at room temperature under extremely humid conditions near 100% relative humidity because of their hygroscopic nature. This situation prompted us to seek for better electrode materials. As a result, Li-based binary carbonate electrodes, Li_2CO_3–MCO_3 (M = Ca, Sr, Ba) were found to be very promising. The use of these electrodes for the NASICON based electrochemical cell not only brings about even better CO_2 sensing properties but also makes the sensor very stable to deliquescence during storage in a highly humid atmosphere at room temperature. Yamazoe et al. reported that solid electrolyte CO_2 sensor

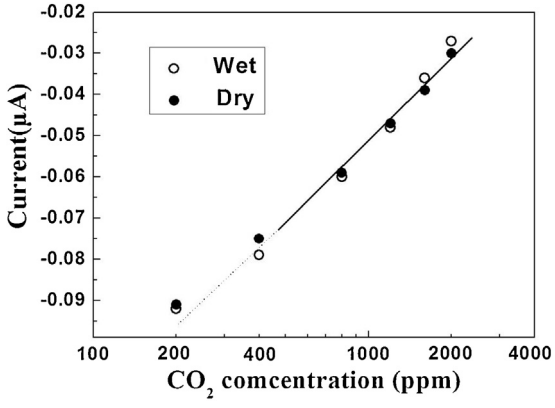

Fig. 4. The amperometric sensor signals as a function of the CO_2 concentration in dry and wet atmospheres. The humid atmosphere was prepared by bubbling air through water at 20 °C (operation voltage = 0.1 V).

Source: reprinted from reference [27] with permission from Elsevier.

was developed by combining NASICON and a Li-based binary carbonate auxiliary electrode represented by Li_2CO_3–$CaCO_3$ (1.8:1 in molar ratio:eutectic mixture) [31]. It responded to CO_2 quickly and reversibly, following a Nernst equation excellently in the CO_2 concentration range 10^2–10^5 ppm. In addition, Li_2CO_3–$CaCO_3$ electrode was found to be stable to deliquescence even when kept under a highly humid condition at 30 °C for more than 700 h. It was found that the electrode using Li_2CO_3–$CaCO_3$ can stand a very humid atmosphere for a considerable span of time, and thus brings about a great ease in the storage and handling of the sensor in practice [31].

The binary systems bring about several advantages such as quick response, resistance to disturbance by water vapor, resistance to deliquescence in storage under humid conditions and capability of operation at lower temperature such as 350 °C. However, the mechanism of such improvements has not yet been understood well. The sensors of this type possess a hetero-junction between the electrolyte (NASICON) and the auxiliary phase (carbonate). It seems that the junction should play an important role on CO_2 sensing performance and its improvement. Miura et al. investigated the devices combining NASICON with a series of Li_2CO_3–$CaCO_3$ binary carbonates for CO_2 sensing properties and the hetero-junction involved to evaluate the role of interfacial structure in this type device [32]. The CO_2 sensing properties and hetero-junction structure of the NASICON-based devices varied rather extensively with the composition of Li_2CO_3–$CaCO_3$ phases used. When pure Li_2CO_3 was used, a thin layer assumed to be Li_2ZrO_3 was formed on the interface between NASICON and carbonate. When Li_2CO_3:$CaCO_3$ (1:2) was used, in contrast, the formation of $CaZrO_3$ layer (30 mm thick) inside NASICON was observed. Surprisingly, the corrosion area containing $CaZrO_3$ increased extensively with decreasing $CaCO_3$ content. The formation of fairly well defined $CaZrO_3$ layer is considered to give the best lower-temperature CO_2 sensing capability to the device using Li_2CO_3:$CaCO_3$ (1:2).

Furthermore, to research the deterioration mechanism of sensors and obtain sensors with better reproducibility and long-term stability, W. Weppner et al. have investigated potentiometric CO_2 sensors based on NASICON. The sensor arrangement may be described as chemical sensor of type III, "(−) Pt (or Au), $Na_{0.9}CoO_2$ |NASICON| Na_2CO_3, Pt (or Au) (+)", with $Na_{0.9}CoO_2$ as reference electrode and Na_2CO_3 as auxiliary or sensing electrode [33]. Comparing with the property of the sensor with structure as "(−) Pt, $Na_{0.9}CoO_2$ | NASICON | carbonate, Pt, O_2, CO_2 (+)" and analyzing the mechanism, the authors got the deterioration reason: Many intermediate compounds such as Na-zirconates, Na-silicates, Na-phosphates, Na-oxides, Si-oxides, etc. with a wide range of stoichiometry may be formed at the two interfaces electrolyte/electrode. Nevertheless, once an intermediate compound involving the electrons from the electronic lead is formed at the interface, this compound contributes to the cell voltage. If the formed intermediate compound is electrically non-conducting, it has the property of a capacitor with a dielectric constant, which influences the measured cell voltage and provides a parallel shift of the voltage. Finally, sensors like (−) Au, $Na_{0.9}CoO_2$ |NASICON| Na_2CO_3, Au (+) showed good reproducibility and long-term stability.

To fabricate reproducible and durable CO_2 sensors, maintenance of a stable and reversible ionic activity in the sensing and reference electrodes is the most important technique. Sadaoka et al. [34] investigated the effects of adding Nd_2O_3 to the Li_2CO_3 layer acting as an auxiliary electrode on the CO_2 sensing characteristics. Fig. 5 shows the EMF (According to IUPAC [35], the name electromotive force and the symbol EMF are no longer recommended. Instead, electric potential difference, ΔV, should be used. However, since this article reviews old figures, we will keep the original denomination electromotive force, EMF, throughout this article.)

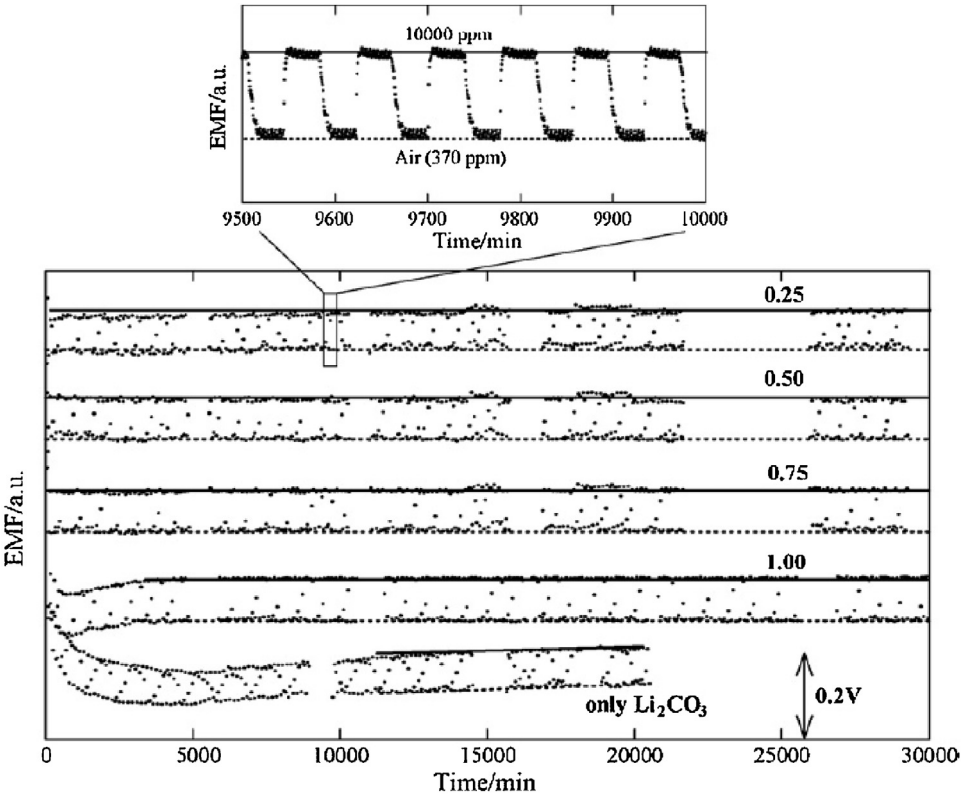

Fig. 5. Carbon dioxide sensing behavior of the sensors at 460 °C. Test gases of 10,000 ppm (solid line) and 370 ppm (dotted line) CO_2 were repeatedly changed. For the auxiliary electrode, the mixture of Li_2CO_3 and Nd_2O_3 was heated in 100% CO_2 gas at 800 °C for 2 h. The mixing molar ratio of $[Li_2CO_3]/[Nd_2O_3]$ as the starting materials is denoted in the figure.

Source: reprinted from reference [34] with permission from Elsevier.

responses of the CO_2 gas sensors using only Li_2CO_3 and heat-treated mixtures of Li_2CO_3 and Nd_2O_3 as an auxiliary electrode [34]. In these measurements, air (370 ppm CO_2 with ambient moisture) and the standard gas (10,000 ppm CO_2) were alternately changed in a 30-min interval. The measurements were started after reaching a designated temperature from room temperature, and then continued for 20–30 days to observe the stability and reversibility of the EMF response. The EMF had a significant drift for the sensor with only Li_2CO_3 as an auxiliary electrode. For the sensor with the heat-treated 1:1 mixture of Li_2CO_3 and Nd_2O_3 as an auxiliary electrode, a similar drift having a decreasing EMF tendency was also observed during the initial short period. To improve the sensing stability, a new auxiliary electrode material based on Li_2CO_3 and Nd_2O_3 was developed.

Brosda et al. developed potentiometric sensor based on screen-printed NASICON films [36]. In this article, it has been proposed that the sintering process of the thick film influences the chemical surface composition of NASICON and as a consequence the response of the sensor. The highest sintering temperature that can be used is limited by the decomposition of NASICON and an increasing thickness of the amorphous layer at the surface, whereas the lowest temperature is limited by the adhesion of the solid electrolyte onto the alumina substrate surface. Therefore the window of sintering temperature is small and covers only the range from 1120 to 1170 °C.

Unlike authors of above literatures that improved the property of CO_2 sensors by altering auxiliary electrode materials, Holzinger et al. [37,38] used Na-β″-Al_2O_3-pellets as a solid electrolyte, Na_2CO_3 as a measuring electrode and a two phase reference electrode consisting of $Na_2Ti_3O_7/Na_2Ti_6O_{13}$ or Na_2Ti6O_{13}/TiO_2. Since the influence of the oxygen partial pressure fixes the activity of the elements on both sides, no oxygen partial pressure dependence of the sensor voltage occurs. Sahner et al. transferred this idea into a fully screen-printed planar sensor device, using NASICON as a solid electrolyte and $Na_2CO_3/BaCO_3$ mixtures as a measuring electrode [39]. They researched the influence of "sodium-rich ($Na_2Ti_3O_7/Na_2Ti_6O_{13}$)" and "sodium-poor ($Na_2Ti_6O_{13}/TiO_2$)" on the performance of sensors. As a result, the observed n values for sensor device with the sodium-rich reference were 2.14 ± 0.06 (total of 4 specimens, each measured 3 times at 500 °C) and 2.12 ± 0.06 (total of 4 specimens at 600 °C). The devices presented a much higher emf reading than expected from the thermodynamic calculations and experimental results. Analyzing the XRD of NASICON and reference electrode materials, the "sodium-rich" composition was found to react with the ion conducting NASICON during thermal treatment. For the thick film sensors using a sodium-poor reference formulation, excellent agreement with the theory was observed. Screen-printed sensor devices were prepared and tested with respect to CO_2 response, reproducibility, and cross-interference of oxygen. After attaching a screen-printed heater, sensor elements were operated actively in a cold gas stream to determine the CO_2 concentration in exhaled air [40].

Recently, Dang et al. also reported the studies on solid electrolyte CO_2 sensors' moisture resistance by altering the reference electrode materials [41]. To overcome this problem, a sensor using a porous $BaCO_3$ film as reference electrode (p-Sensor) was fabricated, a porous $BaCO_3$ film was formed by PMMA doping. For the purpose of comparison, sensor without this porous structure (o-Sensor, i.e. an opened reference electrode) and sensor with a dense $BaCO_3$ film (d-Sensor) also have been fabricated. The authors measured the EMF response to CO_2 as a function of CO_2 concentration under 70%RH conditions. Although the EMF values of both d-sensor and

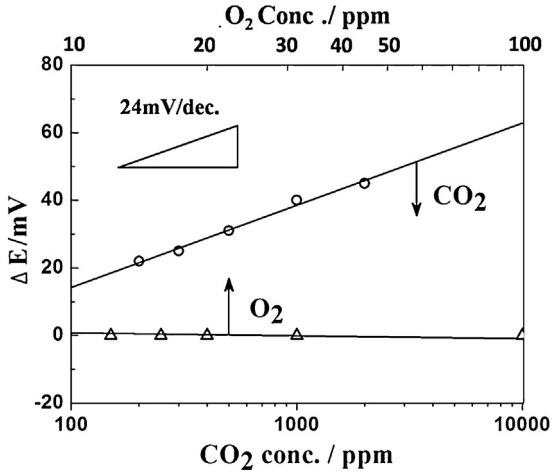

Fig. 6. Sensing performance to CO_2 or O_2 of the open-reference electrode type sensor device at 300 °C, $NdCoO_3$|NASICON|$La_{0.8}Pb_{0.2}CoO_3$.
Source: reprinted from reference [49] with permission from Elsevier.

o-sensor was still very much linear to the logarithm of CO_2 concentration under humid conditions. The observed n values for d-sensor, p-sensor and o-sensor were 1.7, 2.0 and 2.4, respectively. This result suggests that of p-sensor is closer to theoretical value. The reason for the good performance of p-sensor under humid condition was suggested to be due to the almost the same porous structure of both electrodes that make two Pt electrodes potential dependence of RH cancel each other out.

4. Development of NASICON-based mixed-potential type sensors

For above two types of sensors, the long-time stability and moisture resistance need further be improved, due to the hygroscopicity of the oxysalt auxiliary electrode as well as the interface reaction between the oxysalt and NASICON. Unlike these two types of sensors, the mixed-potential-type sensor based on NASICON uses an oxide as a sensing electrode which has good moisture resistance and not directly involved in the electrode reaction (electrode catalyst), so it has been a hot research topic in recent years [48–53,57–64]. The primal research on sensor with the oxide electrode was proposed by S. Bredikhin [48], using SnO_x (doped with Sb, V, etc.) as sensing electrode and Na_xCoO_2 as reference electrode. In this work, non-equilibrium-potential phenomenon was found and the mechanism was discussed briefly. Then, Shimizu et al. developed a CO_2 sensor with perovskite-type oxide electrodes ($NdCoO_3$ and $La_{0.8}Ba_{0.2}CoO_3$ for sensing and reference electrodes). The $NdCoO_3$ and $La_{0.8}Ba_{0.2}CoO_3$ electrodes have high and poor sensitivity to CO_2, respectively, while they have almost the same sensing performance to oxygen. Fig. 6 shows CO_2 and O_2 sensing properties of the open-reference electrode type sensor device at 300 °C [49]. The sensor still has rather good CO_2 sensing properties, while the sensor was hardly affected with oxygen partial pressure, as expected.

Izu et al. [50] fabricated and investigated a planar SO_2 sensor using NASICON as an electrolyte and $V_2O_5/WO_3/TiO_2$ + Au or Pt as a sensing electrode. The planar sensor fabricated by screen-printing is easy to industrialize. In this study, the author varied the vanadium oxide concentration between 1.5 and 3.0 wt% and the electrode materials between Pt and Au and measured the potential changes when exposed to SO_2 and/or other gases in detail. As a result, the sensors using Au electrodes with 1.5 and 3.0 wt% V_2O_5 showed the highest sensitivity with 80–83 mV/decade in the SO_2 range from 20 to 200 ppm was observed at 600 °C. The sensors showed the potential for good selectivity at 600 °C in the case of Au electrodes. The development of this planar sensor not only improves the SO_2 sensor's performance, but laid the foundation for industrialization of the mixed-potential-type sensor.

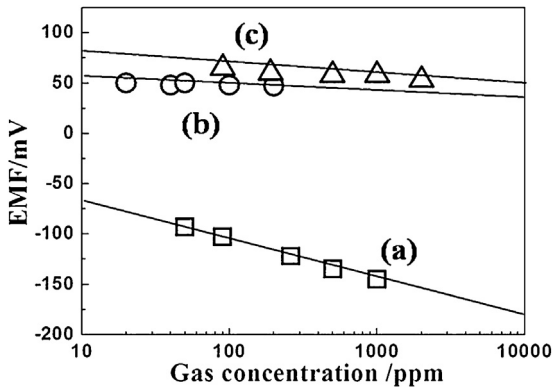

Fig. 7. Sensing performance of the device using $Pb_2Ru_{1.5}Pb_{0.5}O_{7-y}$ electrode to NO in N_2 (a), NO_2 in air (b), and CO_2 in air (c) at 400 °C.
Source: reprinted from reference [53] with permission from Elsevier.

Shimizu et al. [53] developed solid electrolyte electrochemical devices based on NASICON and pyrochlore-type oxide ($Pb_2M_2O_{7-y}$: M = Ir, $Ru_{1-x}Pb_x$; x = 0–0.75) electrodes were found to exhibit good performance for the potentiometric sensing of NO as well as NO_2 at 400 °C. The EMF responses were almost linear to the logarithm of NO or NO_2 concentration. Among the elements tested, the device attached with $Pb_2Ru_{1.5}Pb_{0.5}O_{7-y}$ electrode gave excellent NO sensing properties. Fig. 7 shows dependence of EMF of the sensor device using the $Pb_2Ru_{1.5}Pb_{0.5}O_{7-y}$ and NASICON combination on gas concentration. The sensor hardly responded to NO_2 and CO_2 diluted in air, while it showed high EMF response to NO diluted in N_2, being linear to log P_{NO} with a negative slope of −40 mV/decade [53].

In order to examine the NO_x sensing mechanism, the effect of co-existent oxygen on the measurement of NO concentration was tested for the $Pb_2Ru_{1.5}Pb_{0.5}O_{7-y}$ based device. As shown in Fig. 8 [53], the element showed rather well EMF response to NO co-existed 10% oxygen with linear relationship between EMF versus log P_{NO}. However, the slope of +43 mV/decade was completely different in sign from that for NO in N_2 (Fig. 7(a)). As mentioned above, the sensor signal was largely influenced by the coexisted oxygen. The mixed potential mechanism [54–56] should proceed on the

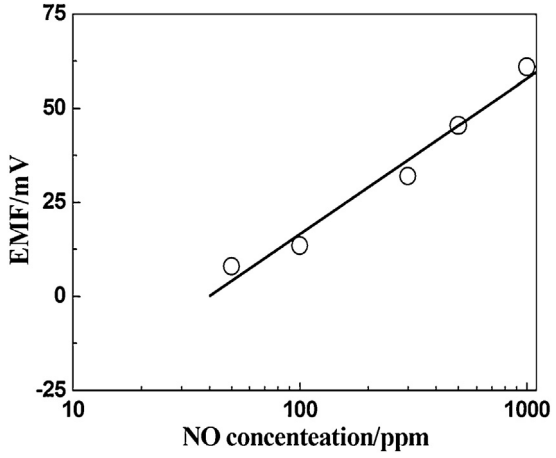

Fig. 8. NO sensing performance of the device using $Pb_2Ru_{1.5}Pb_{0.5}O_{7-y}$ electrode under coexisted oxygen (10%) at 400 °C.
Source: reprinted from reference [53] with permission from Elsevier.

sensing electrode. Therefore, each EMF value could be determined by the potential at which cathodic and anodic reactions proceed at an equal rate. For NO_2 sensing, the following electrochemical reactions (1) and (2) are assumed for the cathodic and anodic reactions, respectively.

$$NO_2 + 2e^- = NO + O^{2-} \quad (1)$$

$$O^{2-} = (1/2)O_2 + 2e^- \quad (2)$$

For NO sensing, the reactions are changed drastically by the coexisted oxygen. When the co-existed oxygen is rare (NO sensing in N_2), reactions (3) and (4) are assumed for the cathodic and anodic reactions, respectively. When a sufficient amount of oxygen is co-existed, reactions (5) and (2) are assumed for the cathodic and anodic reactions, respectively.

$$NO + O^{2-} = NO_2 + 2e^- \quad (3)$$

$$(1/2)O_2 + 2e^- = O^{2-} \quad (4)$$

$$NO + O_2 + 2e^- = NO_2 + O^{2-} \quad (5)$$

Oxygen in reaction (4) should be considered as an impurity (10 ppm O_2) of N_2 gas used. However, the sensing mechanisms of the present electrochemical device still need further investigation [53].

5. Our approaches to develop NASICON-based mixed-potential type sensors attached with oxide electrodes

5.1. Methods

The NASICON was synthesized with $ZrO(NO_3)_2$, $NaNO_3$, $(NH_4)_2HPO_4$ and $Si(C_2H_5O)_4$ by sol–gel process. The sensor was fabricated with an alumina tube of 6 mm long, 0.8 and 1.2 mm in inner and outer diameters. The NASICON precursor was applied on an alumina tube twice and sintered at 900 °C for 6 h in air. Then noble metal (Pt or Au) and oxide layers were formed on the two ends of NASICON layer. Some special sensor structure will be described in the related part in detail.

5.2. Results and discussion

Some results of the NASICON based gas sensors using oxide electrodes were listed in Table 1. As shown in Table 1, for improving the performance of sensors, two main approaches have been utilized: the exploration of new oxide electrode materials and the design of novel sensor structure.

5.2.1. Novel oxide electrode-attached sensors

Some novel oxide electrode materials (Pr_6O_{11}-doped SnO_2, $CaMg_3(SiO_3)_4$-doped CdS, V_2O_5-doped TiO_2, C-doped Cr_2O_3 and ZnO–TiO_2) for sensing H_2S, Cl_2, SO_2, NH_3 and C_7H_8 have been developed.

5.2.1.1. Pr_6O_{11}-doped SnO_2-attached H_2S sensor. We have reported the NASICON based H_2S sensor using Pr_6O_{11}-doped SnO_2 electrode as sensing electrode. Compared with pure SnO_2, Pr_6O_{11}-doped SnO_2 was found to be more suitable for detecting H_2S. Fig. 9 shows that EMF of the device attached with Pr_6O_{11}-doped SnO_2 is perfectly linear to the logarithm of H_2S concentration, and the slopes are 13, 37, 74, 32 and 31 mV/decade at 200, 250, 300, 350 and 400 °C, respectively. With increasing the operating temperature, the slope tended to increase. At 300 °C, the largest value of the slopes occurred, but above 300 °C the slope tended to decrease. This could arise from the consumption of H_2S when it diffused through the Pr_6O_{11}-doped SnO_2 electrode layer at higher temperatures [57].

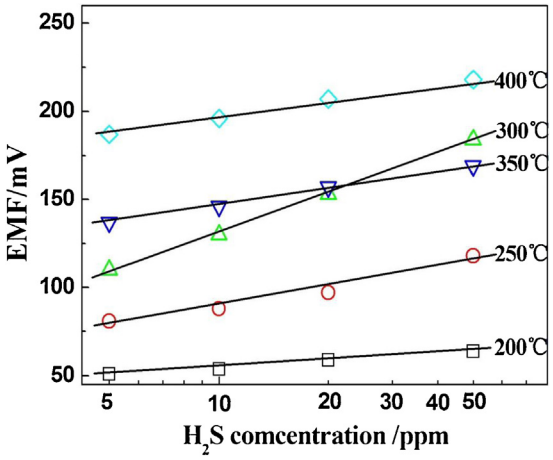

Fig. 9. Dependence of EMF of the sensor attached with Pr_6O_{11}-doped SnO_2 on the H_2S concentration at 200–400 °C.
Source: reprinted from reference [57] with permission from Elsevier.

It was also seen that the sensor showed a good selectivity to H_2S against SO_2, NO_2, CH_4 and CO, and an excellent resistance to water vapor. The sensor had speedy response kinetics to H_2S: the 90% response time to 5, 20 and 50 ppm H_2S was 8, 6 and 4 s, respectively, and the recovery time was 12, 18 and 30 s, respectively. On the basis of XPS analysis for the H_2S-adsorbed sensing electrode, a sensing mechanism involving the mixed potential at the sensing electrode was proposed.

5.2.1.2. $CaMg_3(SiO_3)$-doped CdS-attached Cl_2 sensor. The sensor using $CaMg_3(SiO_3)_4$-doped CdS exhibited excellent sensing properties to 1–10 ppm chlorine in air at 100–250 °C [58]. The sensing properties strongly depended on the sintered temperature of the sensing electrode materials. The dependence of EMF on the Cl_2 concentration for the sensing devices attached with the sensing electrode materials sintering at different temperatures (A: 500 °C, B: 600 °C, C: 700 °C and D: 800 °C) was shown in Fig. 10. For all devices, the EMFs were almost proportional to the logarithm of chlorine concentration, but the device sintered at 600 °C gave the largest sensitivity (slope) to Cl_2. The sensitivity of sensor using $CaMg_3(SiO_3)_4$-doped CdS sintered at 600 °C was −392 mV/decade at 200 °C. The cross-sensitivities of the device attached with B to other various gases, i.e. SO_2, H_2S, NO_2, NH_3, CH_4 and CO each 100 ppm in air, were measured at 200 °C and the results obtained

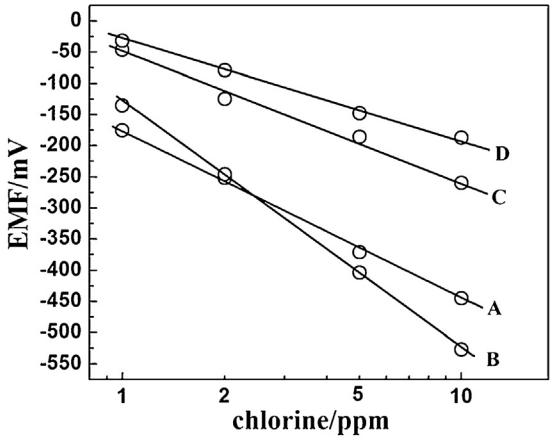

Fig. 10. EMF vs. Cl_2 conc. for sensors calcining at 500–800 °C; A, B, C, and D calcining at 500, 600, 700 and 800 °C, respectively.
Source: reprinted from reference [58] with permission from Elsevier.

Table 1
Typical mixed-potential type gas sensors utilizing NASICON and oxide electrodes.

Gas	Sensor structure air, RE | electrolyte | SE, target gas	Sensitivity (mV/decade)	Gas conc. (ppm)	Operating temperature(°C)	References
H_2S	Air, Au | NASICON | Au, Pr_6O_{11}-SnO_2, H_2S(+air)	74	5–50	300	[57]
Cl_2	Air, Au | NASICON | Au, $Cd_3O_2SO_4$, Cl_2(+air)	−392	1–10	200	[58]
SO_2	Air, Au | NASICON | Au, V_2O_5-TiO_2, SO_2(+air)	−78	1–50	300	[59]
NH_3	Air, Au | NASICON | Au, porous Cr_2O_3, NH_3 (+air)	−89	50–500	350	[60]
C_7H_8	Air, Au | NASICON | Au, ZnO-TiO_2 C_7H_8(+air)	−90	5–50	350	–
NH_3/C_7H_8	NH_3(+air), Cr_2O_3, Au|NASICON| Au, Air, Au | NASICON | Au, ZnO-TiO_2, C_7H_8 (+air)	−91/−60	50–500/5–50	350	[61]
Cl_2	Air, | NASICON | Au | NASICON | Au, Cr_2O_3, Cl_2(+air)	−270	1–50	300	[62]
CO	Air, Pt | NASICON | Au, $NiFe_2O_4$, CO (+air)	−45	100–1000	350	[63]
NO	Air, Au | NASICON | Au, $NiWO_4$ CO (+air)	70	5–500	350	[64]

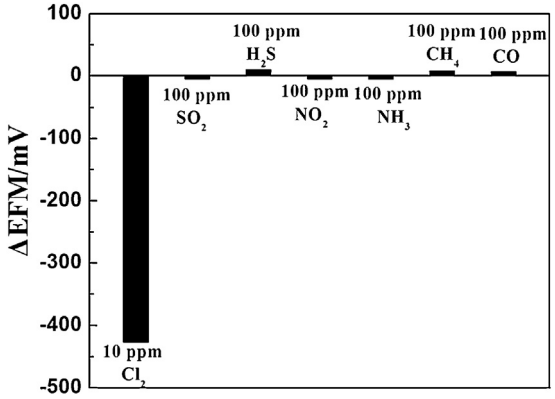

Fig. 11. Cross-EMF responses of the sensor using $CaMg_3(SiO_3)_4$-doped CdS to various gases at 200 °C.
Source: reprinted from reference [58] with permission from Elsevier.

are shown in Fig. 11. The cross-sensitivities were rather small or almost none, indicating its excellent Cl_2 selectivity.

5.2.1.3. V_2O_5–TiO_2-attached SO_2 sensor. A high performance SO_2 sensor was also developed by combining NASICON with V_2O_5-doped TiO_2 sensing electrode [59]. The influence of V_2O_5 doping concentration on the sensing characteristics of the sensor was investigated, and the result was shown in Fig. 12. The variety of EMF of the sensor based on pure TiO_2 to 50 ppm SO_2 was −70 mV at 300 °C and the 90% response and recovery times were 5 and 25 s, respectively. A small amount of V_2O_5 doping (<5 wt%) could largely improve the sensitivity of sensor. When the V_2O_5 doping concentration was 5 wt%, the sensor showed the largest response as well as the fastest response and recovery speeds, the variety of EMF was −176 mV, and the 90% response and recovery times were 10 and 35 s, respectively. However, when the doping concentration of V_2O_5 was increased further, the ΔEMF sharply decreased, and the response and recovery speeds also become slow. The dependence of the sensing performance on V_2O_5 the doping concentration could be explained as following: in the case of the small V_2O_5 doping concentration, V_2O_5 can uniformly be loaded on the surface of TiO_2 with small particle size and show high electrochemical activity to SO_2, inducing high response and speedy response kinetics; in the case of the high V_2O_5 doping concentration, the V_2O_5 particle size can observably grow and even become a single crystal phase, resulting in the decreases of electrochemical activity, the response to SO_2 and the response/recovery speeds. It was also seen that the sensor using 5% V_2O_5–TiO_2showed a good selectivity to SO_2 against NO, NO_2, CH_4, CO, NH_3 and CO_2, as well as speedy response kinetics, as shown in Fig. 13.

5.2.1.4. C-doped Cr_2O_3-attached NH_3 sensor. A high performance NH_3 sensor was also developed by using a porous Cr_2O_3 electrode which was prepared by doping 10% carbon nanotube [60]. The sensor using the porous Cr_2O_3 electrode shows higher sensitivity (slope) to NH_3 at 350 °C, compared to that using Cr_2O_3 particle electrode, as shown in Fig. 14. From SEM images of the porous Cr_2O_3 and the Cr_2O_3 particles, it was seen that a lot of apertures appeared on the surface of the porous Cr_2O_3, this could resulted from that the carbon reacted with the oxygen in the air when it was sintered at high temperature. Therefore, the adsorption and diffusion of ammonia through the porous Cr_2O_3 electrode were much facile than that through the pure Cr_2O_3. This could increase the amount of the ammonia molecule that participated in the

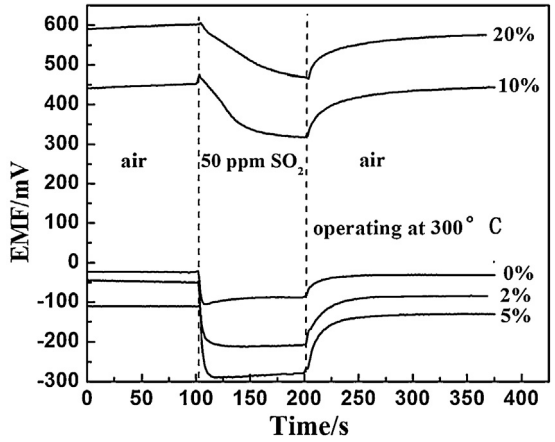

Fig. 12. The influence of V_2O_5 doping on the characteristic of the sensor to 50 ppm SO_2.
Source: reprinted from reference [59] with permission from Elsevier.

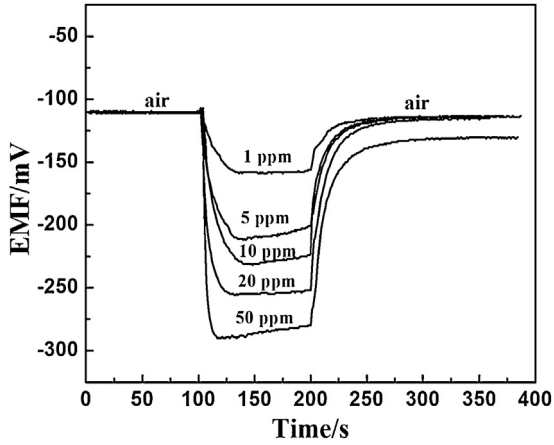

Fig. 13. Response transients of the sensor based on NASICON and V_2O_5-doped TiO_2 sensing electrode to various concentrations of SO_2 at 300 °C.
Source: reprinted from reference [59] with permission from Elsevier.

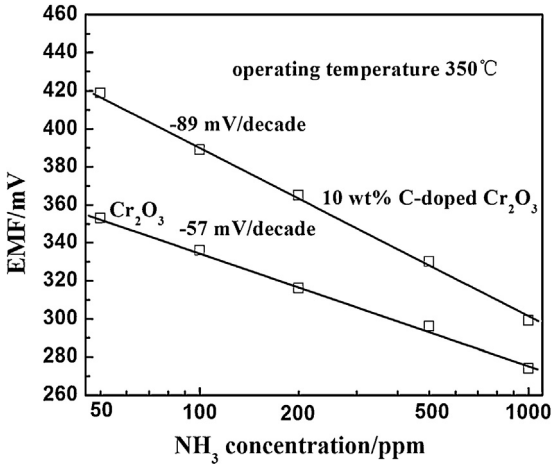

Fig. 14. Dependence of EMF on NH_3 concentration for the sensor attached with the undoped Cr_2O_3 and the 10 wt% C-doped Cr_2O_3.
Source: reprinted from reference [60] with permission from Elsevier.

electrochemical reactions in the triple phase boundary, inducing the sharply increasing of the sensitivity of the sensor to ammonia.

5.2.1.5. ZnO–TiO_2-attached C_7H_8 sensor. In addition, we have developed the NASICON based toluene sensor using ZnO–TiO_2 electrode as sensing electrode. Fig. 15 shows that ΔEMF of the device attached with ZnO–TiO_2 is perfectly linear to the logarithm of C_7H_8 concentration, and the slopes are −40, −90 and −20 mV/decade at 300, 350 and 400 °C, respectively. The sensor had speedy response kinetics to toluene, the 90% response and recovery times to 5, 10, 20 and 50 ppm toluene were 15, 10, 8, 5 s and 25, 39, 50, 90 s, respectively. It was also seen that the sensor showed a good selectivity to toluene.

5.2.2. Sensor with novel structures

In order to improve the sensing performance and realize simple sensor array, we also focused on designing new device structures, such as the dual-function sensor using double oxide electrodes and the buried structure device for blocking the electrochemical reactions on the reference electrode.

5.2.2.1. Sensor with a couple of oxide electrodes. A tubular type sensor utilizing NASICON and a couple of metal oxide sensing electrodes was designed for detecting NH_3 and C_7H_8 simultaneously. The sensor was fabricated using a small alumina tube as shown in Fig. 16 [61]. The C-doped Cr_2O_3 and ZnO–TiO_2 were covered on the mesh-shaped Au electrode at the two ends on the NASICON layer as the sensing electrodes, and the mesh-shaped Au electrode at the central section was used as reference electrode. The thickness of the sensing electrodes was approximately 0.5 mm. Here, C-doped Cr_2O_3 and ZnO–TiO_2 were named as the electrode A and B, respectively, and the corresponding sensors as the sensor A and B. Fig. 17(a) shows the correlations between the EMF and the logarithm of the toluene concentration for the sensors A and B. It could be seen that the sensitivities of sensor A using C-doped Cr_2O_3 sensing electrode to toluene were very small at 250–400 °C. On the other hand, the sensor B using ZnO–TiO_2 sensing electrode exhibited large sensitivities to toluene at 250–400 °C, the slopes were −43, −66, −60 and −42 mV/decade at 250, 300, 350 and 400 °C, respectively. Fig. 17(b) shows the dependence of the EMFs of the sensor with double electrodes on the ammonia concentration. The EMF values of the sensor A and B were almost proportional to the logarithm of the ammonia concentration, and the slopes of the sensor A were much larger than those of the sensor B at any operating temperatures. When the sensor with double electrodes was placed in the toluene atmosphere, due to the large difference of the sensitivities between the sensor B and A at 300 °C, it can selectively detect C_7H_8 at 300 °C. On the other hand, the sensor with double electrodes shows high response to ammonia at 350 °C. Moreover the sensor with double electrodes exhibited well selectivity and rapid response-recovery characteristics to NH_3 and C_7H_8.

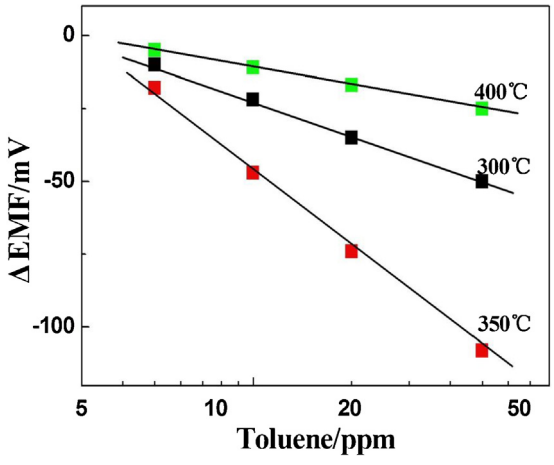

Fig. 15. Dependence of EMF of the sensor attached with ZnO–TiO_2 on the toluene concentration at 300–400 °C.

5.2.2.2. Sensor with buried structure. A buried structure sensing device was developed by using Cr_2O_3 electrode, which can effectively prevent the reaction of the target gas on reference electrode [62]. Fig. 18 shows the dependence of ΔEMF on the Cl_2 concentration for different type of sensing devices (type A: conventional device, type B: simple buried device and type C: deep-buried device), the sensitivity (-slope) for the type C was −270 mV/decade, which is much higher than those for type (A) (−119 mV/decade) and type (B) (−157 mV/decade).This indicated that covered reference electrode with NASICON in Type B and C can block the contact of RE with the Cl_2 and restrain electrochemical reaction in the reference electrode. The sensing response (potential difference between the sensing and reference electrode) as well as the sensitivity of the sensor has been obviously increased. The other way to enhance the sensitivity is to increase the effective area of the sensing electrode. For the sensor A and B, because the sensing electrode and reference electrode were located at both ends of the same NASICON layer, the area of the sensing electrode was reduced to about one half of the surface area of the first NASICON layer. However, for Type C, since the sensing electrode almost covers the all of the surface area of the second NASICON layer (Fig. 18(C)), the area of the sensing electrode is greatly enlarged, and then the sensitivity of the Type C is obviously enhanced.

To discuss the mechanism of mixed-potential, polarization (I–V) curves were measured in the air and Cl_2 with Type C at the concentration of 5 ppm and 10 ppm at 300 °C, respectively. In Fig. 19, the curves measured in the air acted as anodic polarization curves, meanwhile, the value difference between the air and Cl_2 (5 ppm and 10 ppm, respectively) was served as modified cathode polarization curves. Thus, potential difference could be reckoned by the intersection point which was −249 and −332 mV. They were rather close to the measurable value which was −237 and −325 mV. It showed that the mixed-potential mechanism gave an extremely credible explication to the mechanism.

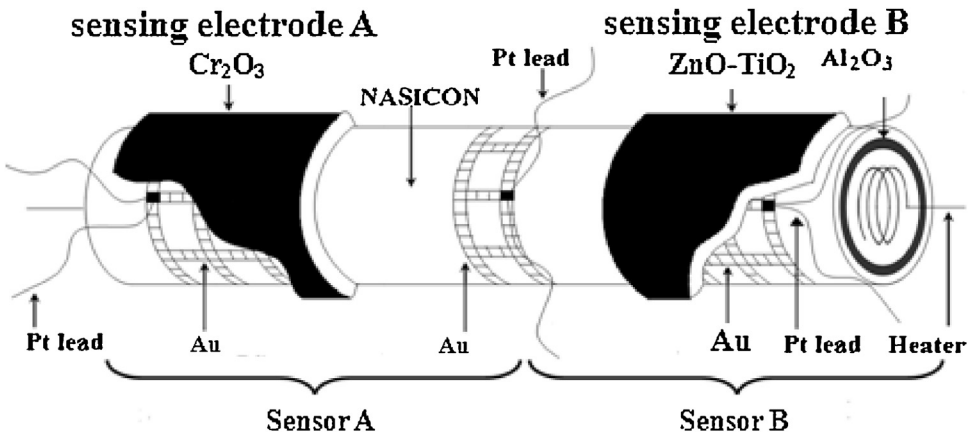

Fig. 16. Structure and response transients of dual-function sensor using Cr_2O_3 and ZnO–TiO_2 for detection of NH_3 and C_7H_8.

5.3. Sensing mechanism of our NASICON-based mixed-potential type sensors

For the sensor based on NASICON and an oxide electrode, the sensing mechanism involved in the mixed potential was proposed [57–61]. Here, as an example, the sensing mechanism of the SO_2 sensor using the V_2O_5-doped TiO_2electrode is described [59]. Firstly, the SO_2 sensor can be expressed with the following electrochemical cell:

$$O_2 \text{ and } SO_2 \text{ in air},\ V_2O_5\text{-doped } TiO_2,\ \text{Au}\,|\text{NASICON}|\,\text{Au},\ O_2 \text{ and } SO_2 \text{ in air} \quad (6)$$

When the SO_2 sensor was exposed to SO_2, a couple of electrochemical reactions (7) and (8) take place at the sensing electrode simultaneously.

$$2Na^+ + SO_2 + O_2{}^+ 2e^- \rightarrow 2Na_2SO_4 \quad (7)$$

$$Na_2O\,(\text{in NASICON}) \rightarrow 2Na^+ + (1/2)O_2 + 2e^- \quad (8)$$

These two electrochemical reactions construct a local cell at the sensing electrode, when the rates of the reactions were equal to each other, they arrive at a dynamic equilibrium, and the electrode potential at the sensing electrode was the mixed potential. By treating Eqs. (7) and (8) with the same process described in [57–61], we could obtain the following equation:

$$E_M = E_0 + \text{mA}\,\ln C_{O_2} - \text{nA}\,\ln C_{SO_2} \quad (9)$$

$$A = \frac{RT}{2(\alpha_1 + \alpha_2)F}$$

Here C_{O_2} and C_{SO_2} are the concentrations of O_2 and SO_2, and E_0, m and n are the constants, F the Faraday constant, R the gas constant and T the absolute temperature, α represent transfer coefficient, respectively. E_M is the electrode potential of the sensing electrode and called a mixed potential. The constants A, n and m changed with the operating temperature. When the concentration of oxygen is fixed, the mixed potential changes linearly with the logarithm of the concentration of SO_2, as described in Eq. (10).

$$E_M = E_0' - \text{nA}\ \ln C_{SO_2} \quad (10)$$

Here, $E_0' = E_0 + \text{mA}\,\ln C_{O_2}$.

Eq. (10) could explain the experimental results very well. Similar reactions also occur at the reference electrode, but since the reference electrode was blocked or had lower activity to the target gases, the response is much smaller than that of the sensing electrode.

For the other sensors based on NASICON and oxide electrodes, similar sensing mechanisms can be applied for explaining their sensing behavior. As for the detail of the sensing mechanism, the further investigation is necessary.

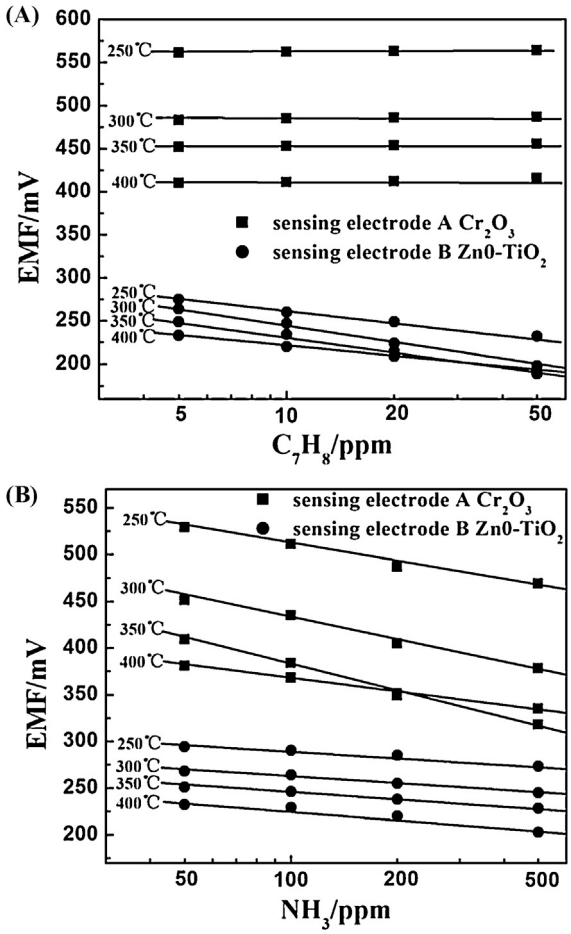

Fig. 17. Sensitivities of the sensor at different temperatures (a) to 5–50 ppm toluene (b) to 50–500 ppm ammonia.

Source: reprinted from reference [61] with permission from Elsevier.

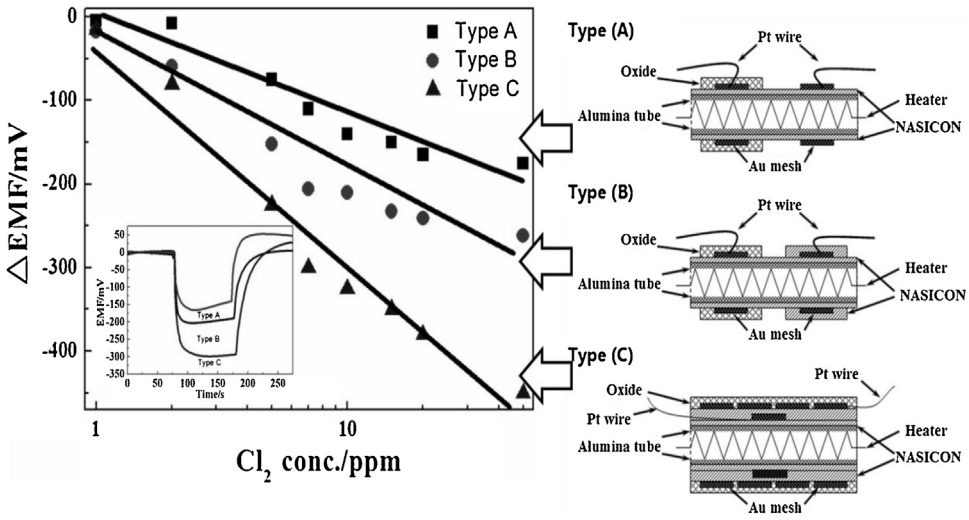

Fig. 18. The buried structure sensor using Cr_2O_3 for detection of Cl_2.

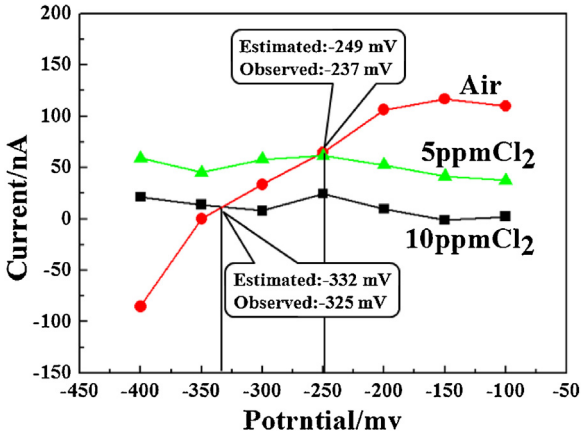

Fig. 19. Polarization curves of Type C measured in the air and Cl_2 (5 ppm and 10 ppm) at 300 °C.

6. Conclusions

The importance of gas sensors using solid electrolytes was fully recognized at an early stage when equilibrium-potential CO_2 sensors using NASICON materialized as a key device for detecting the gases in the atmospheric environment. In recent years, attention has increasingly been paid on new target gases, especially those responsible for global as well as living environmental issues. As demonstrated in this review paper, the mixed potential type sensors utilizing NASICON and oxide electrodes have been developed and showed a potential for detecting the harmful and toxic gases in the atmosphere. For improving the sensing performance of these sensors, two main approaches have been utilized. First, some novel oxide electrode materials have been designed and prepared. Besides the composition of the oxide electrode, the microstructures are very important for the sensing properties, specially, the porosity of the oxide. Second, in order to improve the sensing performance and realize simple sensor array, some novel device structures have been designed, such as the dual-function sensor using double oxide electrodes and the buried structure device for blocking the electrochemical reactions on the reference electrode. In addition, the sensing mechanism related to the mixed potential has been proposed.

In future, this type of sensor is still hope to be applied for the practical monitoring or detecting the environmental gases. Therefore, the development new electrode materials, the design of novel device structure as well as further understanding for the sensing behavior will be focused.

Acknowledgements

Support by NSFC (Nos. 61074172, 61134010, 61104203) and Program for Chang Jiang Scholars and Innovative Research Team in University (No. IRT1017) and Jilin Province Science and Technology Development Plan Program (20106002) is gratefully acknowledged.

References

[1] N. Barsan, M. Hübner, U. Weimar, Conduction mechanisms in SnO_2 based polycrystalline thick film gas sensors exposed to CO and H_2 in different oxygen backgrounds, Sensors and Actuators B 157 (2011) 510–517.
[2] T. Miyata, T. Minami, Chlorine gas sensors with high sensitivity using Mg–phthalocyanine thin films, Applied Surface Science 244 (2005) 563–567.
[3] S. Zhuiykov, N. Miura, Development of zirconia-based potentiometric NO_x sensors for automotive and energy industries in the early 21st century: what are the prospects for sensors, Sensors and Actuators B 121 (2007) 639–651.
[4] N. Miura, G. Lu, N. Yamazoe, H. Kurosawa, M. Hasei, Mixed potential type NO_x sensor based on stabilized zirconia and oxide electrode, Journal of the Electrochemical Society 143 (1996) L33–L35.
[5] N. Miura, H. Kurosawa, M. Hasei, G. Lu, N. Yamazoe, Stabilized zirconia-based sensor using oxide electrode for detection of NO_x in high-temperature combustion-exhausts, Solid State Ionics 86–88 (1996) 1069–1073.
[6] P. Elumalai, V.V. Plashnitsa, T. Ueda, M. Hasei, N. Miura, Dependence of NO_2 sensitivity on thickness of oxide-sensing electrodes for mixed-potential-type sensor using stabilized zirconia, Ionics 12 (2006) 331–337.
[7] J. Park, B.Y. Yooh, C.O. Park, W. Lee, C.B. Lee, Sensing behavior and mechanism of mixed potential NO_x sensors using NiO, NiO(+YSZ) and CuO oxide electrodes, Sensors and Actuators B, Chemical 135 (2009) 516–523.
[8] V.V. Plashnitsa, T. Ueda, P. Elumalai, T. Kawaguchi, N. Miura, Zirconia-based planar NO_2 sensor using ultrathin NiO or laminated NiO–Au sensing electrode, Ionics 14 (2008) 15–25.
[9] N. Miura, S. Yao, Y. Shimizu, et al., High-performance solid-electrolyte carbon dioxide sensor with a binary carbonate electrode, Sensors and Actuators B 9 (1992) 165–170.
[10] J.P. Boilot, P. Salanie, G. Desplanches, D. Le Potier, Phase transformation in $Na_{1+x}Si_xZr_2P_{3-x}O_{12}$ compounds, Materials Research Bulletin 14 (1979) 1469–1477.
[11] D.H.H. Quon, T.A. Wheat, W. Nesbitt, Mater Synthesis, characterization and fabrication of $Na_{1+x}Zr_2Si_xP_{3-x}O_{12}$, Materials Research Bulletin 15 (1980) 1533–1539.
[12] D. Horwat, J.F. Pierson, A. Billard, Magnetron sputtering of NASICON ($Na_3Zr_2Si_2PO_{12}$) thin films part I: limitations of the classical methods, Surface & Coatings Technology 201 (2007) 7013–7017.
[13] D. Horwat, J.F. Pierson, A. Billard, Magnetron sputtering of NASICON ($Na_3Zr_2Si_2PO_{12}$) thin films part II: a novel approach, Surface & Coatings Technology 201 (2007) 7060–7065.

[14] K. Obata, K. Shimanoe, N. Miura, N. Yamazoe, Influences of water vapor on NASICON-based CO_2 sensor operative at room temperature, Sensors and Actuators B 93 (2003) 243–249.
[15] T. Masui, K. Koyabu, S. Tamura, N. Imanaka, Synthesis of a new NASICON-type blue luminescent material, Journal of Alloys and Compounds 418 (2006) 73–76.
[16] A. Essoumhia, C. Favottoa, M. Mansorib, P. Satre, Synthesis and characterization of a NASICON series with general formula $Na_{2.8}Zr_{2-y}Si_{1.8-4y}P_{1.2+4y}O_{12}$ ($0 \le y \le 0.45$), Journal of Solid State Chemistry 177 (2004) 4475–4481.
[17] O. Nakamura, Y. saito, M. Kodama, Y. Yamamoto, Titanium ion substitution ranges for zirconium ion in the$Na_{1+x}Zr2Si_xP_{3-x}O_{12}$ system, Solid State Ionics X9 (1996) 159–164.
[18] M. Barre, M.P. Crosnier-Lopez, F. Le Berre, E. Suard, J.L. Fourquet, Synthesis and structural study of a new NASICON-type solid solution: $Li_{1-x}La_{x/3}Zr_2(PO_4)_3$, Journal of Solid State Chemistry 180 (2007) 1011–1019.
[19] P. Jasifiski, A. Nowakowski, H. Teterycz, K. Wisniewski, Thick film sensor based on NASICON for gas mixture detection, Ionics 5 (1999) 64–69.
[20] P. Jasinski, A. Nowakowski, W. Weppner, Kinetic studies of nasicon based sensors with cyclic voltammetry, Sensors and Materials 12 (2000) 089–097.
[21] K. Frank, H. Kohler, U. Guth, Gas-sensing studies on SnO_2 or NASICON-type composite materials, Ionics 14 (2008) 363–369.
[22] A. Hetznecker, H. Kohler, U. Guth, Enhanced studies on the mechanism of gas selectivity and electronic interactions of SnO_2/Na^+-ionic conductors, Sensors and Actuators B 120 (2007) 378–385.
[23] F. Qiu, L. Sun, X. Li, M. Hirata, H. Suo, B. Xu, Static characteristic of planar-type CO_2 sensor based on NASICON and with an inner-heater, Sensors and Actuators B 45 (1997) 233–238.
[24] N. Miura, M. Iio, G. Lu, N. Yamazoe, Solid-state amperometric NO_2 sensor using a sodium ion conductor, Sensors and Actuators B 35 (36) (1996) 124–129.
[25] N. Miura, M. Ono, K. Shimanoe, N. Yamazoe, A compact solid-state amperometric sensor for detection of NO_2 in ppb range, Sensors and Actuators B 49 (1998) 101–109.
[26] M. Ono, K. Shimanoe, N. Miura, N. Yamazoe, Reaction analysis on sensing electrode of amperometric NO_2 sensor based on sodium ion conductor by using chronopotentiometry, Sensors and Actuators B 77 (2001) 78–83.
[27] J. Lee, J. Lee, S. Hong, Solid-state amperometric CO_2 sensor using a sodium ion conductor, Journal of the European Ceramic Society 24 (2004) 1431–1434.
[28] T. Maruyama, S. Sasaki, Y. Saito, Potentiometric gas sensors for carbon dioxide using solid electrolyte, Solid State Ionics 23 (1987) 107–112.
[29] N. Miura, S. Yao, Y. Shimizu, N. Yamazoe, Carbon dioxide sensor using sodium ion conductor and binary carbonate auxiliary electrode, Journal of the Electrochemical Society 139 (1992) 1384–1388.
[30] S. Yao, Y. Shimizu, N. Miura, N. Yamazoe, Solid electrolyte CO_2 sensor using binary carbonate electrode, Chemistry Letters 1990 (1990) 2033–2036.
[31] S. Yao, S. Hosohara, Y. Shimizu, N. Miura, H. Hutata, N. Yamazoe, Solid electrolyte CO_2 sensor using NASICON and Li-based binary carbonate electrode, Chemistry Letters 1991 (1991) 2069–2072.
[32] T. Kida, H. Kawate, K. Shimanoe, N. Miura, N. Yamazoe, Interfacial structure of NASICON-based sensor attached with Li_2CO_3–$CaCO_3$ auxiliary phase for detection of CO_2, Solid State Ionics 136–137 (2000) 647–653.
[33] W.F. Chu, E.D. Tsagarakis, T. Metzing, W. Weppner, Fundamental, Practical aspects of CO_2 sensors based of NASICON electrolytes, Ionics 9 (2003) 321–328.
[34] H. Aono, Y. Itagaki, Y. Sadaoka, $Na_3Zr_2Si_2PO_{12}$-based CO_2 gas sensor with heat-treated mixture of Li_2CO_3 and Nd_2O_3 as an auxiliary electrode, Sensors and Actuators B 126 (2007) 406–414.
[35] http://goldbook.iupac.org/E01934.html
[36] S. Brosda, H. Wulff, U. Krien, U. Guth, Determination of amorphous layers on thick film NASICON in dependence on different sintering processes, Ionics I (1995) 242–245.
[37] M. Holzinger, J. Maier, W. Sitte, Potentiometric detection of complex gases: application to CO_2, Solid State Ionics 94 (1997) 217–225.
[38] M. Holzinger, J. Maier, W. Sitte, Fast CO_2-selective potentiometric sensor with open reference electrode, Solid State Ionics 86–88 (1996) 1055–1062.
[39] K. Sahner, A. Schulz, J. Kita, R. Merkle, J. Maier, R. Moos, CO_2 selective potentiometric sensor in thick-film technology, Sensors 8 (2008) 4774–4785.
[40] S. Wiegärtner, G. Hagen, J. Kita, R. Moos, M. Seufert, K. Grimmel, A. Bolz, C. Schmaus, A. Kießig, Solid-state potentiometric CO_2-sensor in thick film technology for breath analysis, in: Proceedings of IEEE SENSORS 2011 Conference, October 28–31, 2011, Limerick, Ireland, 2011, pp. 1014–1016, http://dx.doi.org/10.1109/ICSENS.2011.6.
[41] H. Dang, X. Guo, Investigation of porous counter electrode for the CO_2 sensing properties of NASICON based gas sensor, Solid State Ionics 201 (2011) 68–72.
[42] Y. Sadaoka, NASICON based CO_2 gas sensor with an auxiliary electrode composed of $LiCO_3$–metal oxide mixtures, Sensors and Actuators B 121 (2007) 194–199.
[43] T. Kida, K. Shimanoe, N. Miura, N. Yamazoe, Stability of NASICON-based CO_2 sensor under humid conditions at low temperature, Sensors and Actuators B 75 (2001) 179–187.
[44] Q. Zhu, F. Qiu, Y. Quan, Y. Sun, S. Liu, Z. Zou, Solid-electrolyte NASICON thick film CO_2 sensor prepared on small-volume ceramic tube substrate, Materials Chemistry and Physics 91 (2005) 338–342.
[45] S. Baliteau, A-L. Sauvet, C. Lopez, P. Fabry, Characterization of a NASICON based potentiometric CO_2 sensor, Journal of the European Ceramic Society 25 (2005) 2965–2968.
[46] M. Alonso-Porta, R.V. Kumar, Use of NASICON/Na_2CO_3 system for measuring CO_2, Sensors and Actuators B 71 (2000) 173–178.
[47] G.M. Kale, A.J. Davidson, D.J. Fray, Investigation into an improved design of CO_2, sensor, Solid State Ionics 86–88 (1996) 1107–1110.
[48] S. Bredikhim, J. Liu, W. Weppner, Solid ionic conductor rsemicon–ductor junctions for chemical sensors, Applied Physics A 57 (1993) 37–43.
[49] Y. Shimizu, N. Yamashita, Solid electrolyte CO_2 sensor using NASICON and perovskite-type oxide electrode, Sensors and Actuators B 64 (2000) 102–106.
[50] N. Izu, G. Hagen, D. Schönauer, U. Röder-Roith, R. Moos, Planar potentiometric SO_2 gas sensor for high temperatures using NASICON electrolyte combined with $V_2O_5/WO_3/TiO_2$ + Au or Pt electrode, Journal of the Ceramic Society of Japan 119 (2011) 687–691.
[51] S. Kumazawa, N. Miura, N. Yamazoe, Solid electrolyte CO_2 sensor operative at low temperature, extended abstracts of 49th, in: Int. Soc. of Electrochem., Kitakyushu, 1998, p. 903, P-12-15-08.
[52] N. Yamashita, Y. Shimizu, Solid-state CO_2 sensor using NASICON and perovskite-type oxide electrode, Chemical Senses 14 Suppl. B (1998) 189–192.
[53] Y. Shimizu, K. Maeda, Solid electrolyte NOx sensor using pyrochlore-type oxide electrode, Sensors and Actuators B 52 (1998) 84–89.
[54] Y. Shimizu, H. Nishi, H. Suzuki, K. Maeda, Solid-state NO sensor combined with NASICON and Pb–Ru-based pyrochlore-type oxide electrode, Sensors and Actuators B 65 (2000) 141–143.
[55] G. Lu, N. Miura, N. Yamazoe, High-temperature sensors for NO and NO_2 based on stabilized zirconia and spinel-type oxide electrodes, Journal of Materials Chemistry 7 (1997) 1445–1449.
[56] G. Lu, N. Miura, N. Yamazoe, High-temperature hydrogen sensor based on stabilized zirconia and a metal oxide electrode, Sensors and Actuators B, Chemical 35–36 (1996) 130–135.
[57] X. Liang, Y. He, F. Liu, B. Wang, T. Zhong, B. Quan, G. Lu, Solid-state potentiometric H_2S sensor combining NASICON with Pr_6O_{11}-doped SnO_2 electrode, Sensors and Actuators B 125 (2007) 544–549.
[58] X. Liang, F. Liu, T. Zhong, B. Wang, B. Quan, G. Lu, Chlorine sensor combining NASICON with $CaMg_3(SiO_3)_4$-doped CdS electrode, Solid State Ionics 179 (2008) 1636–1640.
[59] X. Liang, T. Zhong, B. Quan, B. Wang, H. Guan, Solid-state potentiometric SO_2 sensor combining NASICON with V_2O_5-doped TiO_2 electrode, Sensors and Actuators B 134 (2008) 25–30.
[60] X. Liang, T. Zhong, H. Guan, F. Liu, G. Lu, B. Quan, Ammonia sensor based on NASICON and Cr_2O_3 electrode, Sensors and Actuators B 136 (2009) 479–483.
[61] X. Liang, G. Lu, T. Zhong, F. Liu, B. Quan, New type of ammonia/toluene sensor combining NASICON with a couple of oxide electrodes, Sensors and Actuators B 150 (2010) 355–359.
[62] H. Zhang, X. Liang, J. Li, G. Lu, NASICON-based potentiometric Cl_2 sensor combining NASICON with Cr_2O_3 sensing electrode, Sensors and Actuators B, Chemical (2012), http://dx.doi.org/10.1016/j.snb.2012.03.024.
[63] X. Liang, S. Yang, T. Zhong, Q. Diao, H. Zhang, J. Li, B. Quan, G. Lu, Mixed potential type carbon monoxide sensor utilizing NASICON and spinel type oxide electrode, Sensor Letters 9 (2011) 832–836.
[64] T. Zhong, X. Liang, H. Zhang, S. Yang, J. Li, B. Quan, G. Lu, Sensing characteristics of potentiometric NO sensor using NASICON and $NiWO_4$ sensing electrode, Sensor Letters 9 (2011) 307–310.

Biographies

Xishuang Liang received the B.Eng. degree from Department of Electronic Science and Technology, Jilin University in 2004. He received his doctor's degree from College of Electronic Science and Engineering of Jilin University in 2009. Now he is a lecturer of Jilin University, China. His current research is on solid electrolyte gas sensor.

Biao Wang received the doctorate degree in electronic sciences in 2008. Now he is an associate professor of Changchun Institute of Optics, Fine Mechanics and Physics, Chinese Academy of Sciences. His current research interests include the software and hardware development of embedded systems.

Han Zhang received the B.Eng. degree from Department of Electronic Sciences and Technology, Jilin University in 2009. He is currently pursuing M.E. Sci. degree in College of Electronic Science and Engineering, Jilin University, China.

Quan Diao received the Bachelor degree in department of Chemistry in 2008. He is currently pursuing Dr. Sci. degree in College of Electronic Science and Engineering, Jilin University, China.

Baofu Quan graduated from Jilin University in 1969. He is a professor of Jilin University, China. His current research is on the characteristics and development of oxide semiconductors (gas sensors material) and solid electrolyte gas sensor.

Geyu Lu received the B.Sci. degree in electronic sciences in 1985 and the M.Sci. degree in 1988 from Jilin University in China and the Dr. Eng. degree in 1998 from Kyushu University in Japan. Now he is a professor of Jilin University, China. His current research interests include the development of chemical sensors and the application of the function materials.